JACC: CARDIOVASCULAR INTERVENTIONS VOL. 2, NO. 3, 2009

ISSN 1936-8798/09/$36.00
PUBLISHED BY ELSEVIER INC. DOI: 10.1016/j.jcin.2008.11.009

# Endothelium-Dependent Vasomotor Dysfunction in Pig Coronary Arteries With Paclitaxel-Eluting Stents Is Associated With Inflammation and Oxidative Stress

Lakshmana K. Pendyala, MD, Jinsheng Li, MD, PHD, Toshiro Shinke, MD, PHD, Sarah Geva, PHD, Xinhua Yin, MD, PHD, Jack P. Chen, MD, FACC, Spencer B. King III, MD, MACC, Keith A. Robinson, PHD, FACC, Nicolas A. F. Chronos, MD, FACC, Dongming Hou, MD, PHD, FACC

*Atlanta, Georgia*

**Objectives** We sought to evaluate coronary epicardial and intramyocardial resistance, arterial vasomotor function, local inflammatory reaction, and superoxide anion ($O_2^{\cdot -}$) production after overlapping paclitaxel-eluting stent (PES) implantation in a porcine model.

**Background** PES implantation has been shown to elicit coronary vasomotor dysfunction. However, underlying mechanisms remain largely unknown.

**Methods** Nine pigs received overlapping PES and bare-metal stents (BMS) in the coronary arteries, and 3 sham animals were naïve. At 1 month, inflammatory response at the overlapped region was assessed by histopathology and scanning electron microscopy. Endothelial vasomotor function and $O_2^{\cdot -}$ at nonstented coronary reference segments were measured by angiography and organ chamber tensiometry, and lucigenin luminometry; vasomotor function of distal resistance arteries was measured by myography.

**Results** Paclitaxel-eluting stents showed reduced late lumen loss, but inflammation and luminal inflammatory cell adherence were higher than for BMS ($p < 0.001$) at overlapped segments. Endothelium-dependent relaxation to substance P was significantly impaired in PES at nonstented coronary reference segments (≥15 mm proximally and distally) and perfusion bed resistance arteries ($p < 0.05$). In contrast, endothelium-independent relaxation to nitroglycerin and sodium-nitroprusside was similar between groups. Local $O_2^{\cdot -}$ production at both proximal and distal nonstented coronary reference segments was elevated for PES when compared with $O_2^{\cdot -}$ production in BMS and naïve arteries ($p < 0.001$).

**Conclusions** Abnormal endothelium-dependent relaxation at both coronary conduit and resistance arteries was demonstrated after overlapping PES implantation. Profound localized inflammatory reaction, as well as enhanced local oxidative stress, may contribute to vasomotor dysfunction. (J Am Coll Cardiol Intv 2009;2:253–62) © 2009 by the American College of Cardiology Foundation

From Saint Joseph's Translational Research Institute/Saint Joseph's Hospital of Atlanta, Georgia. Supported by a Saint Joseph's Translational Research Institute research grant, but contents of the manuscript are solely the responsibility of the authors. Steven Nissen, MD, MACC, served as Guest Editor for this paper.

Manuscript received November 4, 2008, accepted November 5, 2008.

The present generation of paclitaxel-eluting stents (PES) provides dramatic reductions in in-stent restenosis and target lesion revascularization rates compared with these rates in bare-metal stents (BMS) (1–5). However, possible interaction of the potent antiproliferative agent and permanent nonbiodegradable synthetic polymer have raised concerns regarding delayed arterial healing and poor re-endothelialization, which may lead to impaired endothelial function at and adjacent to the stent site (6–8). Overlapping stents are at times required for diffuse and long coronary lesions. The incidence of overlapping stent placement is up to 28% in TAXUS V and VI trials (9,10). Increased local drug concentration and polymer burden at overlapped regions may elicit further delay in vessel recovery especially impaired re-endothelialization.

**Abbreviations and Acronyms**

**BMS** = bare-metal stent(s)
**DES** = drug-eluting stent(s)
**EDdR** = endothelium-dependent relaxation
**EDiR** = endothelium-independent relaxation
**ET** = endothelin
**HEPES** = *N*-(2-hydroxyethyl)-1-piperazine ethanesulfonic acid
**NO** = nitric oxide
**NSRS** = nonstented reference segment
**NTG** = nitroglycerin
**PES** = paclitaxel-eluting stent(s)
**PG** = prostaglandin
**RLU** = relative light unit
**SEM** = scanning electron microscopy
**SMC** = smooth muscle cell
**sP** = substance P

Recently, a growing body of clinical data has shown that compared with BMS, PES implantation may elicit coronary conduit artery vasomotor dysfunction at nonstented reference segments (NSRS) as late as 12 months after implantation (11,12). The mechanism of this phenomenon is still not fully understood. Healthy endothelium generates nitric oxide (NO), which maintains vascular homeostasis and normal vasomotor tone. In pathophysiologic situations, excess generation of reactive free radicals especially superoxide anion ($O_2^{\cdot -}$), may decrease NO bioactivity and bioavailability (13). The resultant impairment of endothelial function is associated with inflammation and thrombogenicity, as well as paradoxical vasoconstriction to acetylcholine or exercise (14).

To date, systematic investigation of vasoreactivity to endothelium-dependent vasodilators in vivo and in vitro following overlapping PES has not been reported. Therefore, in the present study, we aimed to evaluate: 1) inflammatory response at the PES-overlapped region; 2) coronary artery and intramyocardial resistance artery vasomotor function; as well as 3) coronary artery superoxide anion ($O_2^{\cdot -}$) production, 1 month after overlapping PES in porcine coronary model.

## Methods

### Animals and Experimental Protocol

Animal handling and care followed the recommendations of the National Institutes of Health guide for the care and use of laboratory animals and was consistent with guidelines of the American Heart Association. All protocols were approved by the Animal Care and Use Committee and were consistent with Association for Assessment and Accreditation of Laboratory Animal Care guidelines. Twelve juvenile female or castrated male Yorkshire farm pigs (36 ± 1.8 kg) were enrolled in this study.

Twelve animals were used in this study. Six pigs received overlapping stent pairs in each of 2 coronary arteries with randomization to BMS or PES by vessel; adjacent arterial segments were used for vasomotor function and luminometry as shown in Figure 1. Three pigs were normal, unstented age-matched naïve controls, with arterial segments for vasomotor function and luminometry used in the same manner as for stented pigs. Three pigs were used for scanning electron microscopic evaluation of the stent segment luminal surface.

Animals received a combination of 81-mg aspirin and 75-mg clopidogrel by mouth daily for 3 days before stenting and continued until termination. All pigs were fasted overnight before the stent implant procedure. They were sedated by intramuscular injection of ketamine 20 mg/kg, xylazine 2 mg/kg, and atropine 0.05 mg/kg. After intubation, general anesthesia was induced and maintained with isoflurane (2.5%). Electrocardiogram and blood pressure were continuously monitored.

As previously described by our group (15), cardiac catheterization was performed with full heparinization (200 U/kg), and stents were implanted using quantitative coronary angiography guidance to obtain a stent-to-artery diameter ratio ≈1.1:1 to 1.2:1. Overlapping PES (TAXUS, Boston Scientific Corp., Natick, Massachusetts) or BMS (Express 2, Boston Scientific Corp.) were implanted using standard techniques in 9 pigs (2 pairs of overlapping stents per animal). There were no between-groups differences for the total stent length (PES: 26.8 ± 0.4 mm vs. BMS: 26.0 ± 0.6 mm, $p = 0.28$), stent overlap length (PES: 5.2 ± 0.4 mm vs. BMS: 5.1 ± 0.4 mm, $p = 0.85$), or angiographic stent-to-artery diameter ratio (PES: 1.14 ± 0.02 vs. BMS: 1.14 ± 0.01, $p = 0.11$). After late lumen loss measurement and in vivo vascular function studies at 1 month, the animals were terminated.

### Histopathology Analysis

Stented segments for histopathologic analysis were excised and fixed with a mixture of buffered 1.25% glutaraldehyde and 5% formalin. After dehydration in graded ethanol series to 100%, stented vessels were embedded in methyl methacrylate. Sections from the overlapped-stent region were cut using a heavy-duty microtome, collected on glass slides, and stained with hematoxylin-eosin and Movat-Pentachrome. According to previously published methods (16), intramural thrombus (a mixture of fibrin, para-strut amorphous mate-

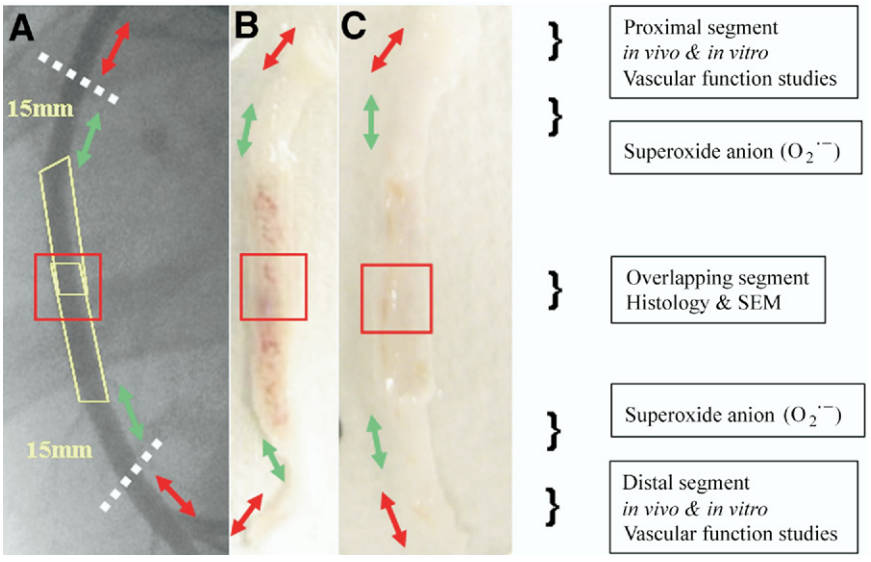


**Figure 1. Macroscopy of the Dissected Coronary Segments With Study Flow Chart**

**(A)** Site of overlapped stented segment **(red box)**; areas of nonstented reference segments used for vasomotor functional testing **(red arrow)**; areas of nonstented segment used for measurement of superoxide **(green arrow)**. **(B)** PES and **(C)** BMS images of isolated coronary stented and nonstented segments used for in vivo and in vitro studies. BMS = bare-metal stent(s); PES = paclitaxel-eluting stent(s); SEM = scanning electron microscopy.

rial and red blood cell debris) and inflammation were scored in all sections: 0 = not present; 1 = mild (scattered); 2 = moderate (encompassing <50% of a strut in at least 25% to 50% of the circumference length); and 3 = severe (surrounding a strut in at least 50% of the circumference length). Similarly, necrosis of the tunica media was also scored: 0 = none; 1 = mild [focal transmural or nontransmural region of medial smooth muscle cell (SMC) necrosis involving any portion of the artery]; 2 = moderate (transmural medial SMC necrosis involving >25% of the circumference of the artery); and 3 = severe (transmural medial SMC necrosis with involvement of >50% of the circumference of the artery).

## Scanning Electron Microscopy Evaluation

Three stents from each PES and BMS group were processed for scanning electron microscopy (SEM) to assess the presence of adherent inflammatory cells on the luminal surface at the overlapped region. The stented vessels were excised into 2 longitudinal hemisections, exposing the coronary luminal surface. Samples were fixed with 2.5% glutaraldehyde, rinsed with cacodylate buffer (pH 7.4), and post-fixed for 1 h in 1% $OsO_4$. After serial ethanol dehydration, the samples were critical-point dried from liquid $CO_2$, attached to aluminum support stubs, and magnetron sputter-coated with ~25-nm gold. Luminal surfaces were examined in a Topcon DS-130 SEM (Topcon Co., Ltd., Tokyo, Japan), and digital images were recorded and assessed. The density of the inflammatory cells was counted in the overlapping region and expressed as cells per square millimeter.

## Vascular Endothelial Function

**Epicardial artery. ANGIOGRAM IN VIVO.** At termination, endothelium-dependent (EDdR) and -independent (EDiR) coronary vasorelaxation responses were assessed after intracoronary infusion of the endothelium-dependent receptor-mediated dilator substance P ([sP] 2 ng/kg) followed by the endothelium-independent vasodilator nitroglycerin ([NTG] 200 $\mu$g) administered via guide catheter. Substance P was infused over 30 s (17). After a 10-min interval, NTG was administered as a bolus. Coronary angiography was performed using identical angiographic projections before and after drug administration. The percent diameter change from baseline to post-infusion was measured at NSRS (1.5 cm proximal and distal to the stent). Vasorelaxation was also measured for the naïve group at similar locations.

**ORGAN CHAMBER APPARATUS IN VITRO.** Hearts were harvested and placed in ice-cold Krebs solution. Coronary artery segments (PES [n = 12], BMS [n = 12], and naïve [n = 6] rings per group, equally divided into proximal and distal) at similar locations as for the in vivo study were cleaned of loose fat and connective tissue. The specimens were then cut into 4-mm long rings and suspended in individual organ chambers (Radnoti Glass Technology, Monrovia, California) filled with 17-ml freshly made Krebs solution with the following composition (millimoles per liter): NaCl 120, $MgSO_4$ 1.17, $KH_2PO_4$ 1.18, $NaHCO_3$

25.0, $CaCl_2$ 2.5, KCl 4.7, glucose 5.5, and 10-μmol/l indomethacin at pH 7.4 (18) and oxygenated with 95% $O_2$ and 5% $CO_2$ at 37°C. Vessel rings were gradually stretched to a basal tension of 4 *g*, which was continuously adjusted over approximately 90 min until stable. Vessels were kept at the same passive tension of 4 *g* throughout the remainder of the study; Krebs buffer was changed every 15 min during the equilibration period.

Contraction was tested with 40- and 100-mmol/l KCl. Rings were then pre-constricted with a single dose (5 μmol/l) of prostaglandin (PG) $F_{2\text{-alpha}}$ until they reached a stable plateau. Then EDdR and EdiR were tested by incremental logarithmic concentrations of sP (0.01 to 100 pmol/l), A23187 (0.03 to 3 μmol/l), and sodium nitroprusside (0.001 to 10 μmol/l). After incubation with 100-μmol/l $N^W$-nitro-L-arginine methyl ester (a competitive inhibitor of NO synthase) for 45 min, sP concentration-response curves were repeated. The rings were then contracted with 0.1-μmol/l endothelin-1 (ET-1) at the end of each experiment. Vessels were washed for 45 min between each concentration-response curve. Isometric tension was digitized, acquired, and analyzed using a Ponemah Tissue Platform System (Gould Instrument System, Valley View, Ohio).

**MYOGRAPH ANALYSIS IN VITRO.** Fifteen microvessel rings (3 naïve, 6 BMS, and 6 PES) harvested 1 month post-stent implantation were studied. Myocardial sections 1.5 × 1.5 cm in size were dissected under a stereomicroscope and resistance arteries (lumen diameter ~250 μm) were isolated. The resistance arteries were sampled in the circulatory distribution of the stented vessel by identifying at least 1 epicardial artery branching from the stented conduit artery, then tracking distal to this branch to obtain the sample. Metal wires (40-μm diameter) were passed through each lumen; 1 wire was mounted on the micrometer and the other on the transducer block side. The vessels were studied in 610M myograph apparatus (Danish Myo Technology, Aarhus, Denmark). Once microvessels were stretched to basal tension of 1 *g*, vasomotor responses were measured in a similar fashion as conduit arteries. Isometric tension was digitized, acquired, and analyzed using a PowerLab system (ADInstruments, Inc., Colorado Springs, Colorado).

### Detection of Oxidative Stress

Superoxide anion ($O_2^{\cdot -}$) production (PES [n = 12], BMS [n = 12], and naïve [n = 6]) rings per group, equally divided into proximal and distal) was estimated by the previously described lucigenin chemiluminescence method (19) with a luminometer (Zylux Corp., Oak Ridge, Tennessee). Proximal and distal NSRS were cut into 4-mm long rings. An assay tube was filled with Krebs–*N*-(2-hydroxyethyl)-1-piperazine ethanesulfonic acid (HEPES) buffer, made by NaCl 99.0, KCl 4.69, $CaCl_2$ 2.5, $MgSO_4$ 1.2, $NaHCO_3$ 25.0, $K_2HPO_4$ 1.03, Na-HEPES 20.0 and glucose 11.1 (mmol/l, pH 7.35), and lucigenin solution with final concentration of 5 μmol/l. Samples were assayed at 37°C in a dark room. Time-dependent output of the luminometer was recorded. Data was expressed in relative light units (RLU) per second for each of the samples; samples were dried at room temperature for 24 h and weighed (milligrams). Final results (in RLU per second per milligram) were calculated as: (Krebs-HEPES plus 5-μmol/l lucigenin reading − Krebs-HEPES reading)/dry weight.

### Statistical Analysis

Data were expressed as mean ± standard error. Statistical analysis was performed by Sigma Stat version 3.5 (Systat Software, Inc., Chicago, Illinois). Comparisons between 2 stent groups or stent and naïve group measurements were performed by the Student paired or unpaired 2-tailed *t* test. A critical value of $p < 0.05$ was considered to indicate significant treatment effect or between-groups difference. The authors had full access to and take full responsibility for the integrity of the data. All authors have read and agree to the manuscript as written.

## Results

### Angiography, Histopathology and SEM Findings in Overlapped Regions

All vessels were angiographically patent at 28 days after implantation. The late lumen loss was significantly reduced for PES (0.46 ± 0.21 mm) in comparison to BMS (1.30 ± 0.16 mm, $p < 0.001$) at overlapped segments.

On gross examination, perivascular adhesions and hemorrhages were found only at the stented segments in PES but not BMS. Under microscopy, a mixture of para-strut fibrin, amorphous material, erythrocyte debris, widespread vessel wall inflammatory cell infiltration, as well as focal medial necrosis beneath the stent struts were evident in the PES group. Histopathologic scoring is shown in Figure 2. Notably, the degrees of inflammation, intramural thrombus, and medial necrosis were all increased in PES compared with BMS at the site of overlapping segments ($p < 0.001$ for all comparisons). For within-group comparison, the inflammation and medial necrosis scores were similar for the nonoverlapped and overlapped segments of PES. However, the intramural thrombosis in the overlapped area was greater than nonoverlapped regions ($p < 0.05$). Inflammatory cells, primarily neutrophils, eosinophils, monocyte-macrophages, as well as giant cells, and such, were noted in neointima of PES. The BMS showed fibrocellular neointima formation with proteoglycan-rich and collagenous matrix, with minimal inflammatory cell infiltration and mild tunica media compression at the site of stent strut contact.

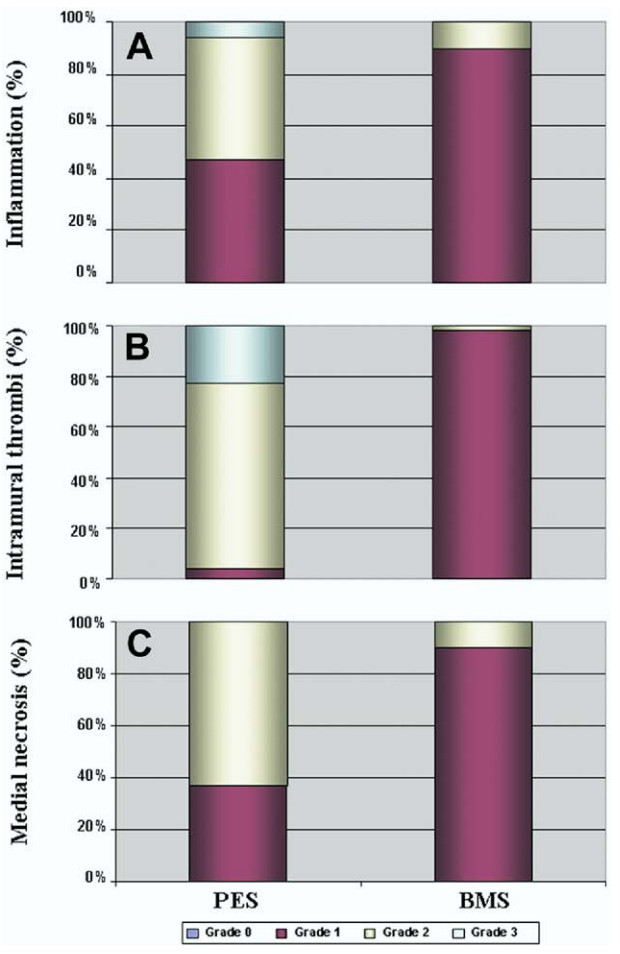


**Figure 2. Histopathologic Scoring**

Stacked column graph showing grading from 0 to 3 in all analyzed sections from each stent type for **(A)** inflammation score, **(B)** intramural thrombi, and **(C)** medial necrosis. In all 3 categories, when compared with BMS, PES showed significant difference ($p < 0.001$ for all 3). Abbreviations as in Figure 1.

In accordance with histopathology scoring, inflammatory cell density on luminal surface at overlapped area assessed by SEM was also markedly increased in PES versus BMS ($1,733 \pm 128/mm^2$ vs. $183 \pm 56/mm^2$, $p < 0.00001$). Representative histological and SEM sections of proximal, overlapped, as well as distal stented segments of PES and BMS are shown in Figures 3 and 4.

## Vascular Endothelial Function

**Angiographic evaluation.** There were no between-groups differences in lumen diameter at baseline for either proximal (PES: 3.07 ± 0.11 mm, BMS: 3.12 ± 0.06 mm, and naïve: 3.00 ± 0.11 mm; p = NS) or distal (PES: 2.98 ± 0.12 mm, BMS: 2.83 ± 0.11 mm, and naïve: 2.83 ± 0.07 mm; p = NS) NSRS. No notable heart rate or mean blood pressure changes were detected after intracoronary injection of either sP or NTG.

Although vasodilation occurred with both sP and NTG, endothelium-dependent diameter change in response to the former was diminished for PES arteries when compared with BMS and naïve arteries. Diameter increase was 0.4 ± 2% for PES (p = 0.007) versus 10 ± 2% for BMS and 15 ± 3% for naïve vessels at proximal NSRS (p = 0.001), with a similar pattern seen at distal NSRS (0.3 ± 3% for PES, p = 0.019; 10 ± 2% for BMS and 15 ± 4% for naïve, p = 0.007). Conversely, NTG-induced EDiR was comparable among PES, BMS, and naïve groups at both proximal (PES: 11 ± 1%, BMS: 12 ± 2%, and naïve: 18 ± 3%; p = NS) and distal (PES: 10 ± 2%, BMS: 14 ± 2%, and naïve: 18 ± 4%; p = NS) NSRS.

**Epicardial conduit artery responses in vitro.** The BMS and naïve arteries relaxed in a dose-dependent manner to sP, a receptor-mediated EDdR (Figs. 5A and 5B). However, for both proximal and distal NSRS, cumulative concentration curves were significantly shifted. The PES vessels showed significantly reduced relaxation at maximal sP concentration compared with relaxation at maximal sP concentration in BMS and naïve vessels (proximal: PES: 38.3 ± 5%, p <

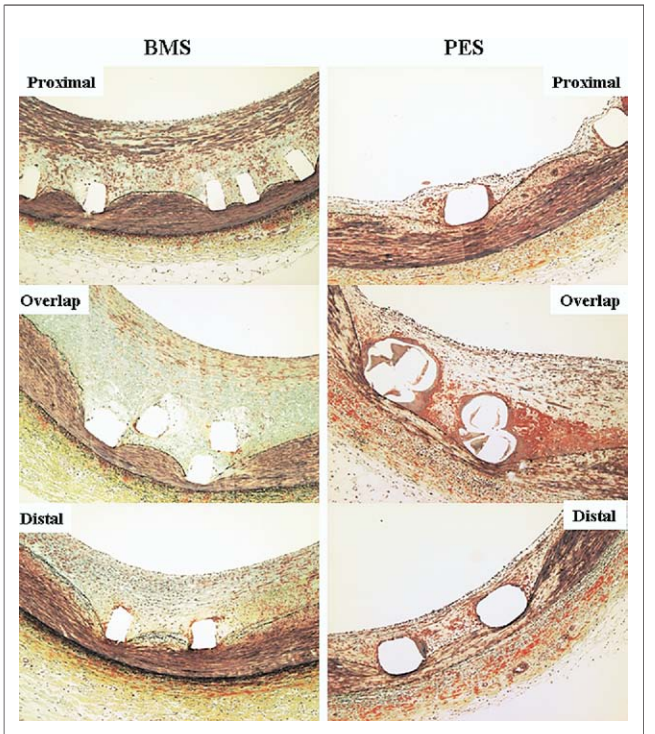


**Figure 3. Histology M-P Staining**

High magnification (100×) microscopic images of M-P–stained sections from proximal, overlapping, and distal sections in PES and BMS demonstrated overall vessel morphologies. Although the neointimal growth was suppressed in PES when compared with BMS, the intramural thrombosis in the overlapped area was greater than in nonoverlapped regions. M-P = Movat-Pentachrome staining; other abbreviations as in Figure 1.

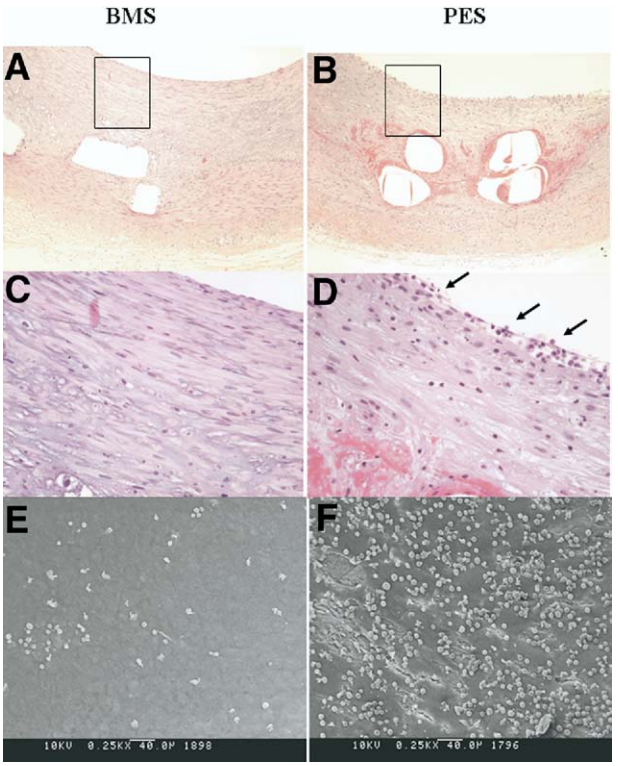


**Figure 4. Histology H&E Staining and SEM**

**(A and B)** High magnification (100×) microscopic images of H&E-stained overlapped sections from coronary segments implanted with PES and BMS. **(C and D)** High magnification (400×) microscopic images of H&E-stained sections of BMS segments exhibited well-healed, thick fibrocellular neointima, completely covered with endothelial or endothelial-like cells. Small amounts of inspissated thrombus and fibrin deposits were observed **(C)**. In PES, drug effect was clearly apparent for all of the overlapping PES in the form of a mixture of para-strut fibrin, amorphous material, and red blood cell debris, as well as widespread inflammatory cell infiltration (several large round mononuclear cells, **black arrows**) into vessel wall and focal medial necrosis beneath the stent struts. **(E and F)** Scanning electron microscopy shows overlapped region for both BMS and PES at 1 month. In contrast to BMS **(E)**, PES **(F)** displayed dramatically more inflammatory cell density on the luminal surface (bar indicates 40 $\mu$m). H&E = hematoxylin-eosin staining; other abbreviations as in Figure 1.

0.05, vs. BMS: 60 ± 7% and naïve: 81.5 ± 2%, $p < 0.001$; distal: PES: 30.9 ± 3%, $p < 0.05$, vs. BMS: 55.7 ± 8% and naïve: 82 ± 2%, $p < 0.001$). The vascular responses of BMS and naïve arteries to calcium-ionophore (A23187, a nonreceptor mediated vasodilator) were similar (proximal: BMS: 83.6 ± 4% vs. naïve: 86.3 ± 2%; p = NS; distal: BMS: 81.5 ± 5% vs. naïve: 84.2 ± 1%, p = NS), whereas the maximal relaxation of the PES group was significantly diminished as compared with relaxation in the BMS and naïve groups (proximal: 57 ± 4%, $p < 0.001$ vs. naïve and BMS; distal: 51.8 ± 7%, $p < 0.05$ vs. naïve and BMS) (Figs. 5C and 5D). Maximal EDiR in reaction to sodium nitroprusside was similar among groups (proximal: PES: 83.9 ± 3% vs. BMS: 90.8 ± 1% and naïve: 93.6 ± 3%, p = NS; distal: PES: 86.4 ± 3% vs. BMS: 85.3 ± 2% and naïve: 92.8 ± 3%, p = NS) (Figs. 5E and 5F). In addition, concentration-dependent relaxation to sP at both proximal and distal NSRS in PES was abrogated by pre-incubation with $N^W$-nitro-L-arginine methyl ester.

Contractile responses to $PGF_{2\text{-alpha}}$ and ET-1 were significantly increased in both proximal and distal PES-NSRS, compared with response in BMS and naïve vessels ($p < 0.001$). The ratio of contraction to ET-1 compared with contraction to 40-mmol/l KCl was greater for PES than for BMS and naïve (proximal: 1.52 ± 0.05 for PES vs. 0.97 ± 0.09 for BMS and 0.85 ± 0.05 for naïve, $p < 0.001$; distal: 3.29 ± 0.58 for PES vs. 1.3 ± 0.10 for BMS and 0.90 ± 0.07 for naïve, $p < 0.001$). Baseline ratio of 5-$\mu$mol/l $PGF_{2\text{-alpha}}$–induced contraction to 40-mmol/l KCl–induced contraction was increased in PES (proximal: 0.70 ± 0.07% for PES, 0.50 ± 0.02% for BMS, and 0.41 ± 0.02% for naïve, $p < 0.001$; distal: 1.03 ± 0.02% for PES, 0.56 ± 0.03% for BMS, and 0.50 ± 0.08% for naïve, $p < 0.001$).

**Myograph analysis of intramyocardial microvascular resistance arteries.** Like epicardial conduit arteries, microvessels in the perfusion bed for BMS and naïve arteries relaxed in a dose-dependent manner to sP (Fig. 6A). However, relaxation response to maximal sP was impaired for PES vessels when compared BMS and naïve vessels (56 ± 11% for PES, $p < 0.05$; 86 ± 6% for BMS and 105 ± 3% for naïve, $p < 0.001$). With calcium-ionophore, relaxation response was reduced in PES compared with naïve (A23187) vessels (65 ± 12% for PES, p = 0.14; 96 ± 15 for BMS and 112 ± 3 for naïve, $p < 0.001$) (Fig. 6B). Maximal EDiR at microvessel level in reaction to sodium nitroprusside was similar among groups (Fig. 6C). Contraction response to ET-1 was similar among the groups.

## Superoxide anion ($O_2^{\cdot -}$) Production of Coronary Conduit Arteries

As shown in Figure 7, overlapping PES implantation at 1 month induced a marked increase in $O_2^{\cdot -}$ production at both proximal and distal NSRS, as measured by lucigenin chemiluminescence (proximal: PES: 36.2 ± 3.3 vs. BMS: 14.6 ± 2., and naïve: 12.4 ± 1.2 RLU/s/mg tissue; $p < 0.001$) and (distal: PES: 77.2 ± 4.0 vs. BMS: 23.2 ± 5.4, and naïve: 19.5 ± 0.6 RLU/s/mg tissue; $p < 0.001$).

## Discussion

Using both in vivo and in vitro methods, we have performed the first systematic evaluation of vasomotor function of coronary epicardial arteries both at proximal and distal NSRS, as well as perfusion bed intramyocardial resistance arteries, after overlapping PES implantation in laboratory

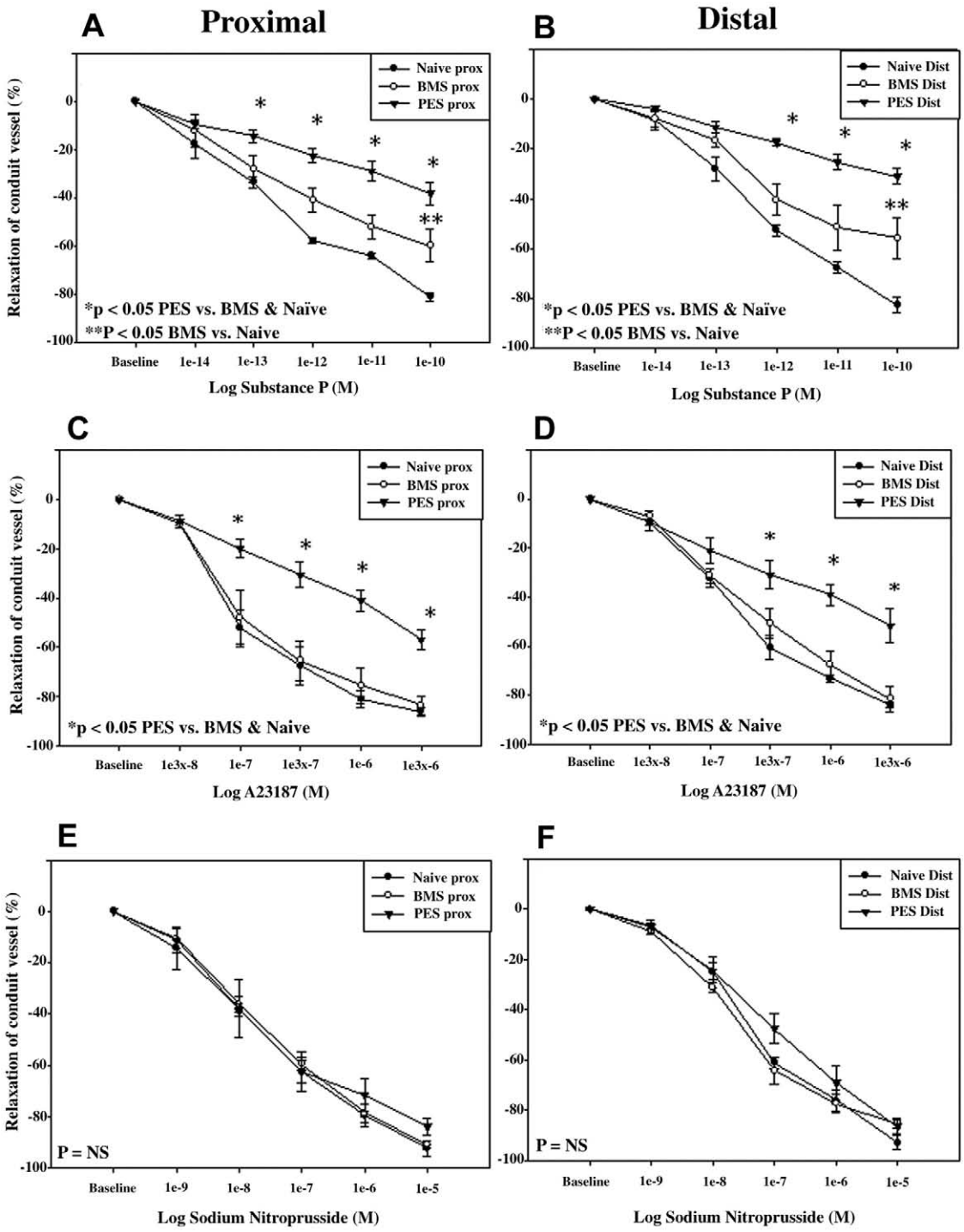


**Figure 5. In Vitro Relaxation Responses of Coronary Segments Proximal and Distal to Stents**

Cumulative concentration-relaxation curves for coronary artery segments proximal and distal to PES and BMS and naïve vessels. **(A and B)** Relaxation to higher concentrations of endothelium-dependent vasodilator sP was inhibited in coronary segments both proximal and distal to PES compared with relaxation in BMS ($p < 0.05$) and naïve ($p < 0.001$) vessels from $10^{-12}$ to $10^{-10}$. **(C and D)** Relaxation to higher concentrations of endothelium-dependent (nonreceptor mediated) vasodilator A23187 was inhibited in coronary segments both proximal and distal to PES compared with relaxation in BMS ($p < 0.001$) and naïve ($p < 0.001$) vessels from $10^{-6}$ to $3 \times 10^{-6}$. **(E and F)** Relaxation to the highest concentration of the endothelium-independent dilator sodium nitroprusside was similar for PES, BMS, and naïve vessels ($p = NS$). sP = substance P; other abbreviations as in Figure 1.

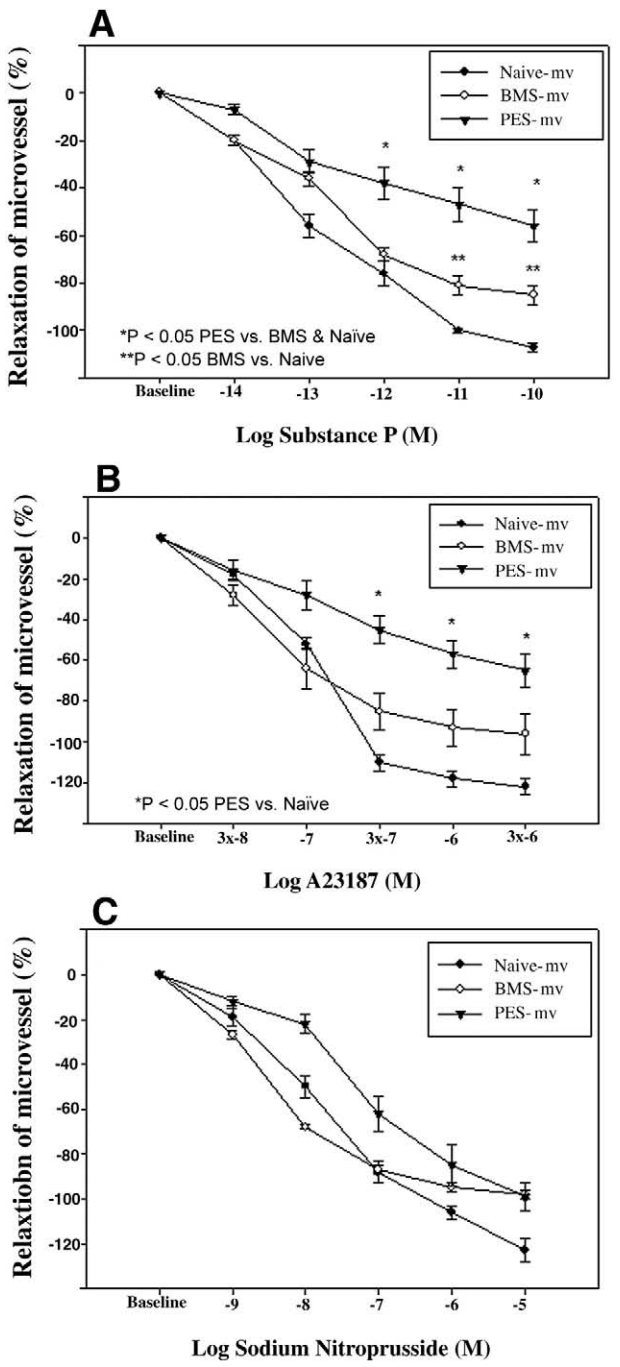


**Figure 6. In Vitro Relaxation Responses of Intramyocardial Resistance Arteries Distal to Stents**

Cumulative concentration-relaxation curves for microvascular arteries distal to PES and BMS, and naïve vessels. **(A)** Relaxation to higher concentrations of endothelium-dependent vasodilator sP was inhibited in PES compared with relaxation in BMS ($p < 0.05$) and naïve ($p < 0.001$) vessels. **(B)** Relaxation to higher concentrations of endothelium-dependent (nonreceptor mediated) vasodilator A23187 was inhibited in coronary segments distal to PES compared with relaxation of naïve vessels ($p < 0.05$). **(C)** Relaxation to the highest concentration of the endothelium-independent dilator sodium nitroprusside was similar for PES, BMS, and naïve vessels ($p$ = NS). Abbreviations as in Figure 1.

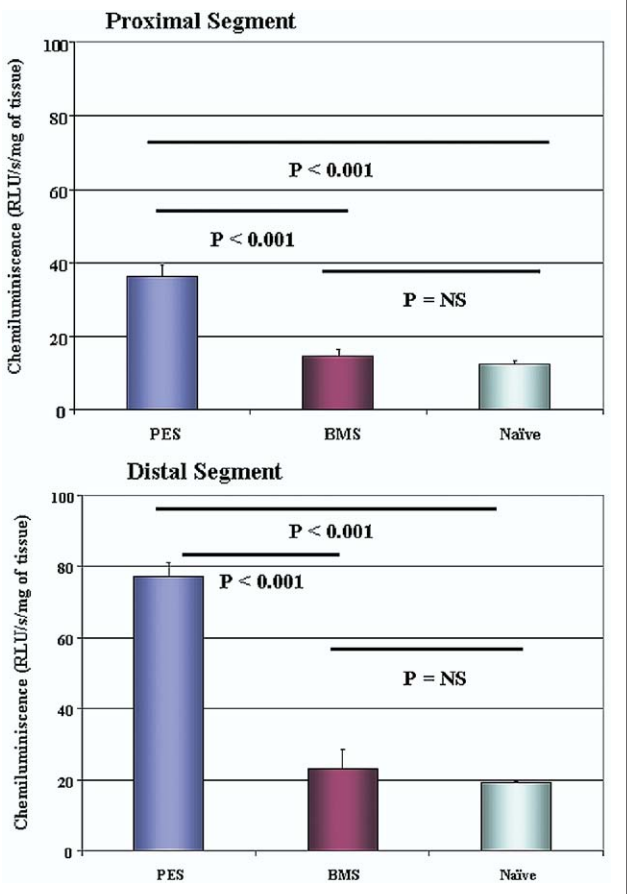


**Figure 7. Superoxide Anion ($O_2^{\cdot -}$) Production Proximal and Distal to the Stent**

Increased $O_2^{\cdot -}$ production at both proximal and distal segments immediately adjacent to stent measured by lucigenin chemiluminescence in PES (proximal: $p < 0.001$; distal: $p < 0.001$) compared with $O_2^{\cdot -}$ production in BMS and naïve vessels (proximal: $p < 0.001$; distal: $p < 0.001$). RLU = relative light units; other abbreviations as in Figure 1.

swine. Additionally, we specifically analyzed the inflammatory response at overlapped region and superoxide anion production at both proximal and distal NSRS. Our data demonstrate that although overlapping PES is effective in inhibiting neointimal growth, a profound adverse effect on vasomotor function was observed in both conduit and resistance arteries distant from the site of direct mechanical injury. Such widespread influence on vasomotor function from the stented coronary artery appears to be associated with extensive localized inflammation at the stent site, as well as increased $O_2^{\cdot -}$ production in the reference coronary arteries.

Consistent with our findings, 2 recent clinical investigations demonstrated that PES implantation was associated with long-term coronary endothelial dysfunction when compared with the BMS counterpart. Togni et al. (11), using exercise-induced flow-mediated EDdR, observed par-

adoxical vasoconstriction response in the peri-stent segments after PES placement at 2 to 12 months, while BMS responses were normal. Similarly, Shin et al. (12) reported both TAXUS and Cypher (sirolimus-eluting) stents showed impairment of EDdR response to acetylcholine in distal and even far distal NSRS at 6 to 9 months. In agreement with our myograph findings, alterations in microcirculation responses following both TAXUS and Cypher implantation were identified; these investigators found that collateral function, measured by collateral flow index, 6 months after drug-eluting stent (DES) was dramatically lower than seen after BMS implantation (20).

Molecular mechanisms of vascular endothelial impairment following DES remain incompletely defined, yet our investigation provides clues into its etiology. Aside from the metal struts, PES contains 2 important components: nonbiodegradable synthetic polymer and paclitaxel. Due to the polymer lipophilicity, only 10% of the initial drug dose can be released from the current slow-release formulation of TAXUS, leaving the residual 90% of the drug in a tissue-bound form (16,21). Multiple factors, including direct toxic effect from the entrapped drug or an acute or delayed hypersensitivity reaction from the polymer and/or drug, may cause DES-triggered vasomotor dysfunction. As recently shown, the vasa vasorum interna in porcine coronary arteries originating directly from the arterial lumen can extend over several centimeters along the coronary artery wall. Therefore, the antiproliferative drug may locally diffuse through vasa vasorum to the NSRS (22,23).

By in vitro cell assay, Axel et al. (24) demonstrated high-dose paclitaxel to be a potent inhibitor of not only SMC, but also of endothelial cell, proliferation and migration. Correspondingly, Farb et al. (25) have shown a dose-dependent decrease in neointimal formation and subsequent increase in vessel wall toxicity from paclitaxel in a porcine coronary model. In the present study, we also confirmed, by histopathology and SEM, that the overlapping PES region (relatively higher doses of drug and polymer) had more pronounced inflammatory and toxic reaction than the BMS and naïve vessels do. It has been demonstrated that increased inflammatory burden is associated with increased production of reactive oxygen species. Kotur-Stevuljevic et al. (26) evidenced that the oxidative stress markers positively correlated with inflammatory markers as a consequence of inflammatory processes in vascular tissue. Superoxide anion, now recognized as a fundamental free radical, is an active participant in oxidative stress states. Oxidative stress via oxygen free radical production, such as superoxide anion, depletes NO reserves, ultimately resulting in endothelial dysfunction (27).

The endothelial permeability barrier is established and maintained primarily by endothelium-to-endothelium junctional structures including adherens junctions, tight junctions, desmosomes, and gap junctions. Recently, $O_2^{\cdot -}$ also has been shown to directly damage the endothelial barrier (28). Many cell types, especially inflammatory cells, are capable of $O_2^{\cdot -}$ generation (29). Passage of macromolecules, including vasoactive peptides, proteins, and other reactive compounds into the arterial tissue, is therefore enhanced in this pathophysiologic scenario.

A notable finding of the present study therefore, and potentially pivotal to the elucidation of DES-associated vasomotor pathophysiology, is the significantly higher level of $O_2^{\cdot -}$ in conduit arteries proximal and distal to PES, compared with levels of $O_2^{\cdot -}$ BMS and naïve vessels. Due to chronically increased production of reactive oxygen species, NO bioavailability may be decreased secondary to inactivation by $O_2^{\cdot -}$, resulting in impairment of endothelium-mediated vascular relaxation response. The importance of NO for EDdR also was confirmed in our experiment by the complete blockage of vasorelaxation in the presence of endothelial NO synthase blockade by $N^W$-nitro-L-arginine methyl esterin PES. Thus, underlying direct drug toxicity and/or polymer incompatibility, potentiation of superoxide activity may be a culprit mechanism to endothelial dysfunction.

Beyond vasorelaxation dysfunction, our data also illustrated significantly increased contractile response to PG $F_{2\text{-alpha}}$ and ET-1 in the both the proximal and distal NSRS for PES. This paradoxical vasoconstrictive response in NSRS may potentially lead to stasis of coronary blood flow, which has been well-documented in clinical case studies (30). The potential contribution of such flow impairment to DES thrombosis is unknown but should be more extensively evaluated in future studies.

**Study limitations.** First, animal models do not precisely simulate responses to DES in humans. Normal porcine coronary arteries are not representative of the diseased human coronary system, which consists of lipid-rich atherosclerotic and potentially thrombotic stenotic lesions. Second, longer-term studies are needed to address potential endothelial functional recovery at later time points. Finally, the relatively small number of animal subjects should be considered when interpreting these results.

## Conclusions

Although the PES were effective in reducing neointima formation, profound adverse effects were noted on vasomotor function involving arterial segments both proximal and distal to the stent at the coronary conduit artery level. Microcirculatory dysfunction was also noted in the perfusion distribution of the stented segment in the form of impaired relaxation. Oxidative stress from increased free radical production is likely an underlying mechanism for conduit artery endothelial dysfunction.

**Acknowledgments**

The authors thank Cindy Baranowski and Lian Dorsey for their expert technical assistance with the histologic section preparation; Ashley Strong, DVM, Jourdan Davis, RVT, and Sheila Wideman for assistance with stent implant procedures; Courtnye Billingsley for project management; Addrena Taylor for her assistance with necropsy and tissue preparation; and Jeannette Taylor of the Robert Apkarian Microscopy Facility of Emory University for scanning electron microscopy.

**Reprint requests and correspondence:** Dr. Dongming Hou, Saint Joseph's Translational Research Institute/Saint Joseph's Hospital of Atlanta, 5673 Peachtree Dunwoody Road, Suite 675, Atlanta, Georgia 30342. E-mail: dhou@sjha.org.

## REFERENCES

1. Morice MC, Serruys PW, Sousa JE, et al. A randomized comparison of a sirolimus-eluting stent with a standard stent for coronary revascularization. N Engl J Med 2002;346:1773–80.
2. Moses JW, Leon MB, Popma JJ, et al. Sirolimus-eluting stents versus standard stents in patients with stenosis in a native coronary artery. N Engl J Med 2003;349:1315–23.
3. Stone GW, Ellis SG, Cox DA, et al. A polymer-based, paclitaxel-eluting stent in patients with coronary artery disease. N Engl J Med 2004;350:221–31.
4. Stone GW, Ellis SG, Cannon L, et al. Comparison of a polymer-based paclitaxel-eluting stent with a bare metal stent in patients with complex coronary artery disease: a randomized controlled trial. JAMA 2005; 294:1215–23.
5. Dawkins KD, Grube E, Guagliumi G, et al. Clinical efficacy of polymer-based paclitaxel-eluting stents in the treatment of complex, long coronary artery lesions from a multicenter, randomized trial: support for the use of drug-eluting stents in contemporary clinical practice. Circulation 2005;112:3306–13.
6. Joner M, Finn AV, Farb A, et al. Pathology of drug-eluting stents in humans: delayed healing and late thrombotic risk. J Am Coll Cardiol 2006;48:193–202.
7. Luscher TF, Steffel J, Eberli FR, et al. Drug-eluting stent and coronary thrombosis: biological mechanisms and clinical implications. Circulation 2007;115:1051–8.
8. Finn AV, Nakazawa G, Joner M, et al. Vascular responses to drug eluting stents: importance of delayed healing. Arterioscler Thromb Vasc Biol 2007;27:1500–10.
9. Ellis SG, Colombo A, Grube E, et al. Incidence, timing, and correlates of stent thrombosis with the polymeric paclitaxel drug-eluting stent: a TAXUS II, IV, V, and VI meta-analysis of 3,445 patients followed for up to 3 years. J Am Coll Cardiol 2007;49:1043–51.
10. Weissman NJ, Ellis SG, Grube E, et al. Effect of the polymer-based, paclitaxel-eluting TAXUS Express stent on vascular tissue responses: a volumetric intravascular ultrasound integrated analysis from the TAXUS IV, V, and VI trials. Eur Heart J 2007;28:1574–82.
11. Togni M, Raber L, Cocchia R, et al. Local vascular dysfunction after coronary paclitaxel-eluting stent implantation. Int J Cardiol 2007;120: 212–20.
12. Shin DI, Kim PJ, Seung KB, et al. Drug-eluting stent implantation could be associated with long-term coronary endothelial dysfunction. Int Heart J 2007;48:553–67.
13. Lavi S, Yang EH, Prasad A, et al. The interaction between coronary endothelial dysfunction, local oxidative stress, and endogenous nitric oxide in humans. Hypertension 2008;51:127–33.
14. Landmesser U, Hornig B, Drexler H. Endothelial function: a critical determinant in atherosclerosis? Circulation 2004;109:II27–33.
15. Shinke T, Li J, Chen JP, et al. Incidence of intramural thrombus after overlapping paclitaxel-eluting stents: angioscopic and histopathologic analysis in porcine coronary arteries. Circulation Interv 2008;1:28–35.
16. Shinke T, Geva S, Pendyala L, et al. Low-dose paclitaxel elution by novel bioerodible sol-gel coating on stents inhibits neointima with low toxicity in porcine coronary arteries. Int J Cardiol 2008 Aug 9 [E-pub ahead of print].
17. Ohwada T, Saito T, Saitoh S, et al. Specificity of vascular reactivity and remodeling after repeated endothelial injury in a swine model. Int Heart J 2006;47:297–310.
18. Li J, Jabara R, Pendyala L, et al. Abnormal vasomotor function of porcine coronary arteries distal to sirolimus-eluting stents. J Am Coll Cardiol Intv 2008;1:279–85.
19. Mohazzab KM, Kaminski PM, Wolin MS. NADH oxidoreductase is a major source of superoxide anion in bovine coronary artery endothelium. Am J Physiol 1994;266:H2568–72.
20. Meier P, Zbinden R, Togni M, et al. Coronary collateral function long after drug-eluting stent implantation. J Am Coll Cardiol 2007;49: 15–20.
21. Pendyala L, Jabara R, Shinke T, et al. Drug-eluting stents: present and future. Cardiovasc Hematol Agents Med Chem 2008;6:105–15.
22. Hofma SH, van der Giessen WJ, van Dalen BM, et al. Indication of long-term endothelial dysfunction after sirolimus-eluting stent implantation. Eur Heart J 2006;27:166–70.
23. Gössl M, Rosol M, Malyar NM, et al. Functional anatomy and hemodynamic characteristics of vasa vasorum in the walls of porcine coronary arteries. Anat Rec Part A 2003;272:526–37.
24. Axel DI, Kunert W, Göggelmann C, et al. Paclitaxel inhibits arterial smooth muscle cell proliferation and migration in vitro and in vivo using local drug delivery. Circulation 1997;96:636–45.
25. Farb A, Heller PF, Shroff S, et al. Pathological analysis of local delivery of paclitaxel via a polymer-coated stent. Circulation 2001;104:473–79.
26. Kotur-Stevuljevic J, Memon L, Stefanovic A, et al. Correlation of oxidative stress parameters and inflammatory markers in coronary artery disease patients. Clin Biochem 2007;40:181–7.
27. Quyyumi AA, Dakak N, Andrews NP, et al. Nitric oxide activity in the human coronary circulation. Impact of risk factors for coronary atherosclerosis. J Clin Invest 1995;95:1747–55.
28. Aslan M, Ryan TM, Townes TM, et al. Nitric oxide-dependent generation of reactive species in sickle cell disease. Actin tyrosine induces defective cytoskeletal polymerization. J Biol Chem 2003;278: 4194–204.
29. MacPherson JC, Comhair SA, Erzurum SC, et al. Eosinophils are a major source of nitric oxide-derived oxidants in severe asthma: characterization of pathways available to eosinophils for generating reactive nitrogen species. J Immunol 2001;166:5763–72.
30. Brott BC, Anayiotos AS, Chapman GD, Anderson PG, Hillegass WB. Severe, diffuse coronary artery spasm after drug-eluting stent placement. J Invasive Cardiol 2006;18:584–92.

**Key Words:** endothelial function ■ paclitaxel-eluting stent ■ inflammation ■ oxidative stress.